DALTON
FULL PAPER

Reaction of $CH_2(Ph_2PSe)_2$ (dppmSe_2) with $[Ru_3(CO)_{12}]$. Fluxional behaviour of $[Ru_3(\mu_3\text{-}Se)_2(CO)_7(\mu\text{-dppm})]$ and crystal structures of $[Ru_4(\mu_4\text{-}Se)_2(\mu\text{-}CO)(CO)_8(\mu\text{-dppm})]\cdot MeOH$ and $[Ru_6(\mu_3\text{-}Se)_4(CO)_{12}(\mu\text{-dppm})_2]\cdot CH_2Cl_2$

Daniele Cauzzi,[a] **Claudia Graiff,**[a] **Giovanni Predieri,***[a] **Antonio Tiripicchio**[a] **and Carlo Vignali**[b]

[a] *Dipartimento di Chimica Generale ed Inorganica, Chimica Analitica, Chimica Fisica,*
Università di Parma, Centro di Studio per la Strutturistica Diffrattometrica del C.N.R.,
Viale delle Scienze, I-43100 Parma, Italy. E-mail: predieri@ipruniv.cce.unipr.it
[b] *Centro Interdipartimentale di Misure 'G. Casnati', Università di Parma, Viale delle Scienze,*
I-43100 Parma, Italy

Received 7th September 1998, Accepted 12th November 1998

The reaction of $[Ru_3(CO)_{12}]$ with dppmSe_2 afforded the open-triangular *nido* cluster $[Ru_3(\mu_3\text{-}Se)_2(CO)_7(\mu\text{-dppm})]$ **1**, the *closo*-octahedral species $[Ru_4(\mu_4\text{-}Se)_2(\mu\text{-}CO)(CO)_8(\mu\text{-dppm})]$ **2** and the cubane-like cage $[Ru_4(\mu_3\text{-}Se)_4(CO)_{10}(\mu\text{-dppm})]$ **3**. Multinuclear NMR data indicated a fluxional behaviour for **1** in solution consisting both in the reversible migration of a metal–metal bond in the cluster and in the oscillation of the methylene group of the dppm ligand. Pyrolysis of **1** gave the condensation derivative $[Ru_6(\mu_3\text{-}Se)_4(CO)_{12}(\mu\text{-dppm})_2]$ containing a central 64-electron butterfly core.

The reaction of tertiary phosphine chalcogenides R_3PE (E = S, Se or Te) with metal carbonyl complexes provides a simple, one-step synthetic procedure to form phosphine-substituted chalcogenido clusters through oxidative transfer of selenium atoms to low-valent metal centres.[1] This method, which takes advantage of the frailty of the P=E bond, affords clusters of different nuclearity, $[M_xE_y(PR_3)_z]$, depending on which combination of metal and phosphine is used. The availability of these clusters offers the opportunity to test whether they are suitable molecular precursors for the production of extended inorganic solids like $M_xE_yP_z$ by mild thermal treatment. The control over the stoichiometric ratio, combined with the kinetic control, which derives from low activation energies of these processes, could allow the synthesis of otherwise inaccessible solid phases or microinhomogeneous materials such as nanocomposites.[2]

Despite the synthetic potential of the phosphine selenides, their reactions with metal carbonyls have been explored only to a limited extent prior to the last three years and, in general, most of the previously described chalcogenido–carbonyl clusters containing Group 15 donor ligands had been obtained by substitution reactions.[3]

As regards chelating diphosphine selenides, we have recently found that the reactions of $[Fe_3(CO)_{12}]$ with three diphosphine diselenides dppmSe_2, dppeSe_2 and dppfcSe_2 produce the substituted 50-electron, *nido* clusters $[Fe_3(\mu_3\text{-}Se)_2(CO)_7\{\mu\text{-}(Ph_2P)_2R\}]$ (R = CH_2, dppm; R = CH_2CH_2, dppe; R = $(C_5H_4)_2Fe$, dppfc) as the main products.[4] These carbonyl clusters have a square-pyramidal structure with two iron and two selenium atoms alternating in the basal plane and the third iron atom at the apex of the pyramid. In spite of their different bites, all the three dppm, dppe and dppfc diphosphines bridge the two non-bonded iron atoms, producing a certain degree of deformation in the cluster core Fe_3Se_2, which appears to depend on the $P\cdots P$ span. The short-bite dppm ligand pushes the basal iron atoms to approach, in such a way that a fluxional motion takes place in solution consisting of the reversible migration of a metal–metal bond from a side of the open triangle to the basal plane (Scheme 1).[4]

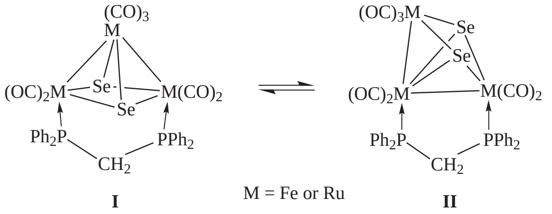

Scheme 1

Considering the ruthenium species, we have observed that the diphosphine diselenide $(Ph_2PSe)_2CH_2$ (dppmSe_2) reacts in toluene with $[Ru_3(CO)_{12}]$ to give the *nido* cluster $[Ru_3(\mu_3\text{-}Se)_2(CO)_7(\mu\text{-dppm})]$ **1** (the expected primary product), the *closo*-octahedral species $[Ru_4(\mu_4\text{-}Se)_2(\mu\text{-}CO)(CO)_8(\mu\text{-dppm})]$ **2** and $[Ru_4(\mu_3\text{-}Se)_4(CO)_{10}(\mu\text{-dppm})]$ **3** [dppm = $(Ph_2P)_2CH_2$], which is the first reported 72-electron Ru–Se cubane-like cage complex.[5] Analogous *nido* and *closo* clusters have been obtained by Woollins and co-workers by treating $(Ph_2PSe)_2NH$ with $[Ru_3(CO)_{12}]$.[6]

This paper, which represents the completion of our previous report,[5] deals both with the fluxional behaviour of **1** in solution, and with the descriptions of the crystal structures of the methanol solvate of $[Ru_4(\mu_4\text{-}Se)_2(\mu\text{-}CO)(CO)_8(\mu\text{-dppm})]$ **2**·MeOH and of the dichloromethane solvate of $[Ru_6(\mu_3\text{-}Se)_4(CO)_{12}(\mu\text{-dppm})_2]$ **4**·CH_2Cl_2, an unusual hexanuclear cluster derived from **1** upon thermal treatment under decarbonylation conditions.

Experimental

General

The starting reagents $[Ru_3(CO)_{12}]$, Se and the diphosphine $(Ph_2P)_2CH_2$ were pure commercial products (Aldrich and Fluka) used as received. The ligand dppmSe_2 was prepared according to literature methods by reaction of elemental Se with dppm.[7] The solvents (C. Erba) were dried and distilled by standard techniques before use. All manipulations (prior to the TLC separations) were carried out under dry nitrogen by means of standard Schlenk-tube techniques. Elemental (C, H) analyses were performed with a Carlo Erba EA 1108 automated analyzer. The IR spectra (KBr discs or CH_2Cl_2 solutions) were recorded on a Nicolet 5PC FT spectrometer, ^1H, ^{13}C, ^{31}P (81.0 MHz; 85% H_3PO_4 as external reference) and ^{77}Se [38.2 MHz; Ph_2Se_2 in $CHCl_3$ (+461 ppm relative to Me_2Se) as external reference] NMR spectra, for $CDCl_3$ solutions, on Bruker instruments AC 300 (^1H and ^{13}C) and CXP 200 (^{31}P and ^{77}Se).

Preparations

Reaction of $[Ru_3(CO)_{12}]$ with dppmSe_2. The compounds $[Ru_3(CO)_{12}]$ (105 mg, 0.16 mmol), Me_3NO (13 mg, 0.16 mmol) and dppmSe_2 (90 mg, 0.16 mmol) were allowed to react in refluxing toluene (90 cm^3) for 1.5 h under a nitrogen atmosphere. The resulting dark red solution was evaporated to dryness and the residue dissolved in a small amount of CH_2Cl_2. Three products were separated by TLC on silica, using CH_2Cl_2–light petroleum, b.p. range 50–70 °C, (2:1) as eluant: $[Ru_3(\mu_3\text{-}Se)_2(CO)_7(\mu\text{-dppm})]$ **1** (20%, red band, R_f 0.9), $[Ru_4(\mu_4\text{-}Se)_2(\mu\text{-}CO)(CO)_8(\mu\text{-dppm})]$ and $[Ru_4(\mu_3\text{-}Se)_4(CO)_{10}(\mu\text{-dppm})]$ **2** and **3** (5 and 14% respectively, brownish yellow band, R_f 0.8). Complexes **2** (light brown) and **3** (light orange), having nearly the same R_f, were separated by fractional crystallization by slow diffusion of methanol in a dichloromethane solution, at about 4 °C. Complex **1**: IR [CH_2Cl_2, ν(CO), cm^{-1}] 2066, 2052, 2007 and 1956; ^1H NMR: δ 3.37 (t, 2 H, CH_2, isomer **I**), 3.98 [dt, 1 H, CH_2, J(HP) 10.6, J(HH) 14, isomer **II**] and 4.68 [dt, 1 H, CH_2, J(HP) 10.6, J(HH) 14 Hz, isomer **II**]; ^{13}C NMR: δ 35.7 [t, J(CP) 30, isomer **I**] and 47.3 [t, J(CP) 30 Hz, isomer **II**]; ^{31}P NMR: δ 57.2 (s, isomer **I**), 20.7 [d, J(PP) 40, isomer **II**] and 14.2 [d, J(PP) 40 Hz, isomer **II**]; ^{77}Se NMR: δ −121 [t, J(SeP) ≈14, isomer **I**], 128 [d, J(SeP) ≈14, isomer **II**] and 126 [d, J(SeP) ≈14 Hz, isomer **II**]. Complex **2**: IR [CH_2Cl_2, ν(CO), cm^{-1}] 2046, 2014 and 1969; ^{31}P NMR δ 23.4 (s). Complex **3**: IR [CH_2Cl_2, ν(CO), cm^{-1}] 2091, 2076, 2027, 2003 (sh) and 1964; ^1H NMR δ 4.17 [t, 2H, CH_2, J(HP) 11.5 Hz]; ^{31}P NMR δ 9.4 (s). Calc. for $C_{35}H_{22}O_{10}P_2Ru_4Se_4$: C, 30.4; H, 1.60. Found: C, 29.8; H, 1.9%.

Pyrolysis of $[Ru_3(\mu_3\text{-}Se)_2(CO)_7(\mu\text{-dppm})]$ 1. Cluster **1** was refluxed in toluene, under a nitrogen atmosphere, in the presence of an equimolar amount of Me_3NO, until (1 h) the IR spectrum of the mixture showed decisive changes in the carbonyl region. The deep reddish brown solution was evaporated to dryness and the residue dissolved in a small amount of CH_2Cl_2. Three products were separated by TLC on silica, using CH_2Cl_2–light petroleum (2:1) as eluant: unchanged **1** (46%), the *closo* cluster **2** (19%), and the new hexanuclear species $[Ru_6(\mu_3\text{-}Se)_4(CO)_{12}(\mu\text{-dppm})_2]$ **4** (10%, red), which was recrystallized by slow diffusion of methanol in a dichloromethane solution, at about 4 °C. Complex **4**: IR [CH_2Cl_2, ν(CO), cm^{-1}] 2023s, 2006w, 1983m and 1858w; ^1H NMR δ 3.86 [dt, 2 H, CH_2, J(HP) 12, J(HH) 12] and 3.58 [dt, 2 H, CH_2, J(HP) 12, J(HH) 12 Hz]; ^{31}P NMR δ 55.1 [d, J(PP) 78] and 37.6 [d, J(PP) 78 Hz]. Calc. for $C_{62}H_{44}O_{12}P_4Ru_6Se_4$: C, 36.7; H, 2.19. Found: C, 36.3; H, 2.3%.

X-Ray crystallography

The crystallographic data for the compounds **2**·MeOH and **4**·CH_2Cl_2 are summarized in Table 1. Accurate unit cell parameters were obtained by using the setting angles of 30 high-angle reflections; no significant decay was noticed over the time of data collection for all compounds. Intensities were corrected for Lorentz-polarization effects. A correction for absorption[8] was applied (maximum and minimum value for the transmission coefficient 1.0000 and 0.6318 for **2**·MeOH, 1.0000 and 0.7768 for **4**·CH_2Cl_2).

Both structures were solved by Patterson methods using SHELXS 86.[9] The structure of compound **2**·MeOH was refined by full matrix least squares based on F_o using the SHELX 76 program,[10] first with isotropic thermal parameters and then with anisotropic thermal parameters for all non-hydrogen atoms. The structure of compound **4**·CH_2Cl_2 was refined by full matrix least squares based on F_o^2 using the SHELXL 93 program,[11] first with isotropic thermal parameters and then with anisotropic thermal parameters for all non-hydrogen atoms except for the atoms of solvent molecules. In both structures the hydrogen atoms were placed at their geometrically calculated positions (C–H = 0.96 Å) and refined "riding" on the corresponding carbon atoms. The final cycles of refinement were carried out on the basis of 479 variables for **2**·MeOH, 812 for **4**·CH_2Cl_2. The biggest remaining peak in the final difference map was equivalent to about 1.56 e $Å^{-3}$ for **4**·CH_2Cl_2, 1.05 e $Å^{-3}$ for **2**·MeOH. All calculations were carried out on the GOULD POWERNODE 6040 and ENCORE 91 computers of the Centro di Studio per la Strutturistica Diffrattometrica del C.N.R., Parma.

CCDC reference number 186/1247.

Results and discussion

The reaction of $[Ru_3(CO)_{12}]$ with dppmSe_2 affords a variety of products, three of which could be isolated by preparative TLC: the *nido*-cluster $[Ru_3(\mu_3\text{-}Se)_2(CO)_7(\mu\text{-dppm})]$ **1**, the *closo*-octahedral species $[Ru_4(\mu_4\text{-}Se)_2(\mu\text{-}CO)(CO)_8(\mu\text{-dppm})]$ **2** and the cubane-like cage $[Ru_4(\mu_3\text{-}Se)_4(CO)_{10}(\mu\text{-dppm})]$ **3**, whose crystal structure was described in a previous paper.[5]

Cluster **1** has the well known bicapped open-triangular 50-electron core (Scheme 1) and is the expected primary product of the oxidative attack of dppmSe_2 on the starting carbonyl cluster. Its structure in the solid state is expected to be the same as those observed for other phosphine disubstituted Ru_3Se_2 derivatives[1e,3a,6] and for the iron analogue $[Fe_3(\mu_3\text{-}Se)_2(CO)_7(\mu\text{-dppm})]$,[4] which exhibit the two P donor groups coordinated to the two non-bonded, basal metal atoms.

Nevertheless, its NMR spectra in solution suggest a fluxional behavior similar to that exhibited by the iron analogue and depicted in Scheme 1. In fact, as illustrated in Fig. 1, the ^{31}P spectrum shows a singlet (δ 57.2, 36%) and two doublets at lower frequency [δ 20.7 and 14.2, J(PP) 40 Hz, 64%]. This pattern is identical to that of the iron derivative and is consistent with the proposed dynamic behaviour, which consists of the migration of a metal–metal bond induced by the diphosphine ligand. In contrast to the iron case (T_c 360 K) however, coalescence occurs at a temperature higher than 370 K. Other examples of mobility of metal–metal bonds in clusters have recently been reported by Rauchfuss and co-workers.[12]

The ^1H NMR pattern is more complex than that of the iron analogue displaying three sets of peaks: a triplet at δ 3.37 (corresponding to the ^{31}P singlet) and two equally populated pseudo-quartets [dt, J(HH) 14, J(HP) 10.6] centered at δ 3.98 and 4.68 (corresponding to the ^{31}P doublets); they are correlated by chemical exchange as indicated by an EXSY experiment, and give coalescence at 325 K in toluene, the estimated $\Delta G^\ddagger$ value being 12 kcal mol^{-1}. This pattern is indicative of a further dynamic behaviour involving the CH_2 group of the diphosphine, when it bridges two bonded ruthenium atoms; it is represented in Scheme 2, emphasizing the non-equivalence of the two methylene protons. Consequently, the two selenium atoms experience different environments and, accordingly, the ^{77}Se NMR spectrum (Fig. 1) shows two sets of peaks: (i) two multiplets, probably doublets [δ 126 and 128, J(SeP) ≈14 Hz] due to two non-equivalent selenido ligands, only one J(PSe) being apparently detectable, (ii) a triplet at δ −121 which corresponds to the ^{31}P singlet, as deduced by multinuclear selective irradiation experiments.

It is interesting that the fluxional behaviour involving the CH_2 group, described above, occurs at a rate suitable to be detected by NMR spectroscopy, at room temperature, only in

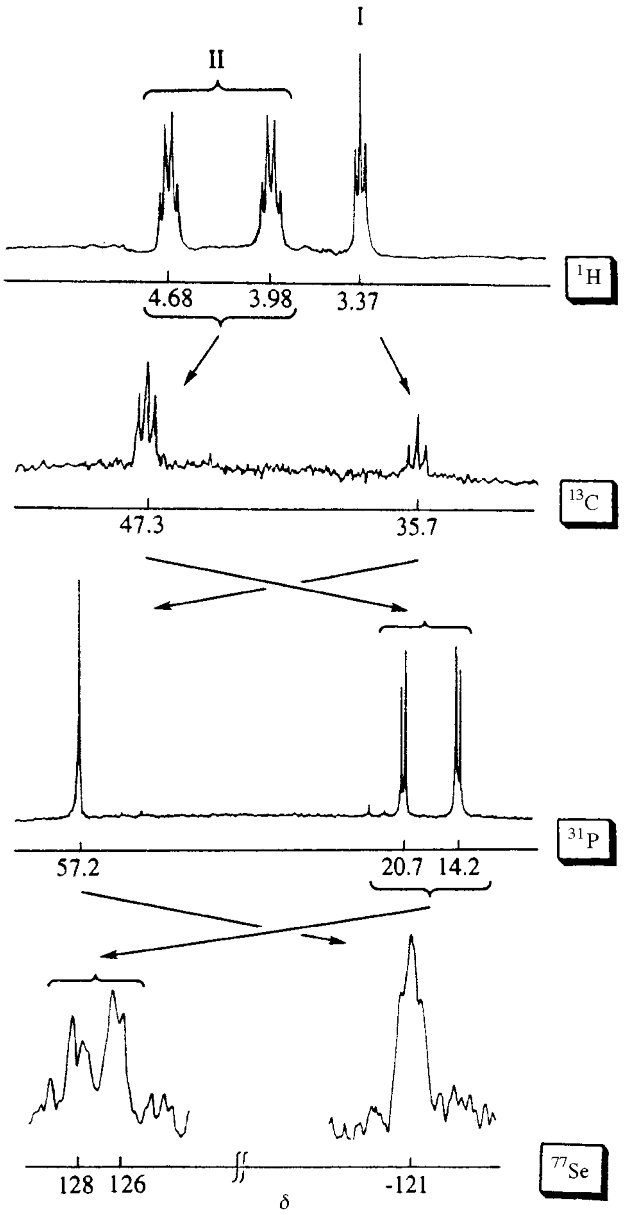

Fig. 1 The NMR spectra of compound **1**, evidencing the presence of the two isomeric forms **I** and **II** depicted in Scheme 1.

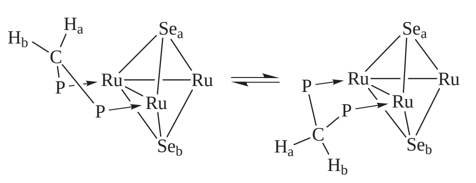

Scheme 2

the case of the ruthenium derivative **1,** when dppm bridges two bonded ruthenium atoms (isomer **II** of Scheme 1). In the other configuration present in solution (dppm bridging two non-bonded basal metal atoms) and in both configurations of the iron analogue the exchange rate appears too high to allow the observation of two different hydrogen and selenium atoms.

Fig. 2 shows the structure of **2** together with the atomic numbering system. Selected bond distances and angles are given in Table 2. The cluster adopts a *closo*-octahedral geometry with seven skeletal electron pairs, being practically isostructural with $[Ru_4(\mu_4\text{-}Se)_2(\mu\text{-}CO)(CO)_8\{(R_2P)_2NH\text{-}P,P'\}]$ (R = Ph or Pr^i),[6] and with $[Ru_4(\mu_4\text{-}Te)_2(\mu\text{-}CO)(CO)_8(\mu\text{-}dppm)]$.[3d] The diphosphine and a carbonyl ligand symmetrically bridge two opposite edges of the Ru_4 square plane (maximum deviation from the Ru_4 mean plane is 0.04 Å), resulting in a shortening of the relevant Ru–Ru bond distances [Ru(1)–Ru(2) 2.793(1), Ru(3)–Ru(4) 2.772(1) Å] with respect to the other two [2.855(1) and 2.852(1) Å]. It is interesting that, in contrast to the PPh_3-monosubstituted[13] and disubstituted[1e] Ru_4Se_2 *closo*-octahedral derivatives (exhibiting two quasi-symmetrical bridging carbonyls), cluster **2** contains only one symmetrically bridging CO [Ru(3)–C(7) 2.051(6), Ru(4)–C(7) 2.042(5) Å] which practically lies on the Ru_4 mean plane [deviation of C(7) 0.014 Å].

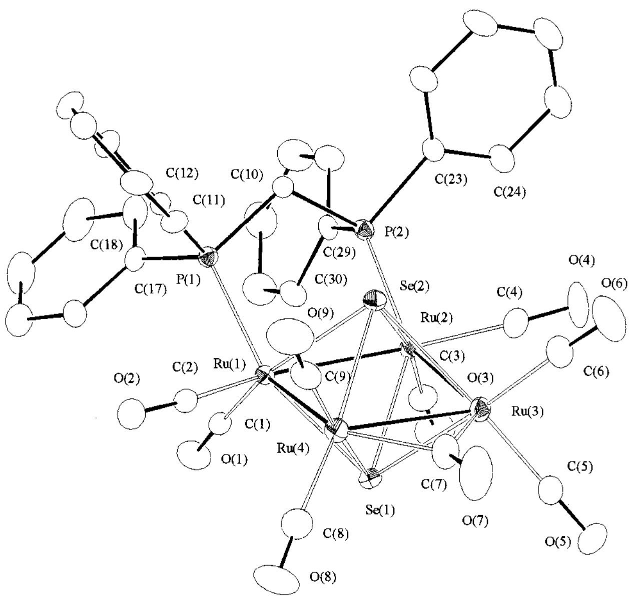

Fig. 2 View of the molecular structure of $[Ru_4(\mu_4\text{-}Se)_2(\mu\text{-}CO)(CO)_8\text{-}(\mu\text{-}dppm)]$ **2** together with the atomic numbering system.

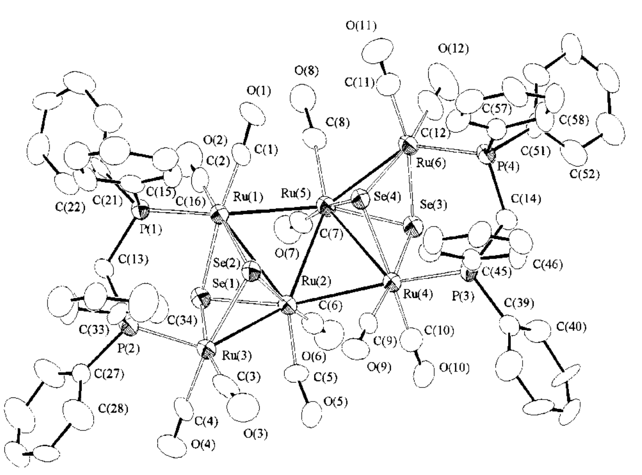

Fig. 3 View of the molecular structure of $[Ru_6(\mu_3\text{-}Se)_4(CO)_{12}\text{-}(\mu\text{-}dppm)_2]$ **4** together with the atomic numbering system.

The dppm ligand is co-ordinated in such a way that the angle between the Ru_4 and P_2Ru_2 [Ru(1)–P(1) 2.304(1), Ru(2)–P(2) 2.341(1) Å] mean planes is 137.1(1)°. The short-bite ligand geometry of dppm [P(1)–C(10)–P(2) 115.2(2)°, P(1) $\cdots$ P(2) 3.105(2) Å] does not permit the P atoms to occupy the transoid positions with respect to Se(1) as observed in the PPh_3 substitution derivatives:[1e,13] the P(1)–Ru(1)–Se(1) and P(2)–Ru(2)–Se(1) angles are 155.5(1) and 144.5(1)° respectively. The resulting co-ordination geometries around Ru(1) and Ru(2) place C(2) and C(4) in the neighborhood of Ru(4) and Ru(3) respectively [Ru(4) $\cdots$ C(2) 2.92(1) and Ru(3) $\cdots$ C(4) 2.84(1) Å], suggesting weak bridging interactions. The chalcogen atoms Se(1) and Se(2) lie respectively 1.643(1) below and 1.643(1) Å above the Ru_4 mean plane, the eight Ru–Se distances ranging between 2.544(1) and 2.626(1) Å.

A series of C–H $\cdots$ O interactions contributes to packing,

Table 1 Summary of crystallographic data for compounds **2**·MeOH and **4**·CH_2Cl_2

	2·MeOH	**4**·CH_2Cl_2
Formula	$C_{34}H_{22}O_9P_2Ru_4Se_2$·$CH_3OH$	$C_{62}H_{44}O_{12}P_4Ru_6Se_4$·$CH_2Cl_2$
M	1230.73	2112.04
Crystal system	Monoclinic	Monoclinic
Space group	$P2_1/c$	$P2_1/c$
Radiation (λ/Å)	Mo-Kα (0.71073)	Cu-Kα (1.54184)
a/Å	15.526(3)	19.262(4)
b/Å	14.372(2)	18.413(3)
c/Å	17.852(4)	20.534(5)
β/°	93.72(1)	106.01(2)
V/Å^3	3975(1)	7000(3)
Z	4	4
D_c/g cm^{-3}	2.029	2.004
F(000)	2328	4056
Crystal size/mm	0.18 × 0.32 × 0.38	0.15 × 0.28 × 0.31
μ(Mo-Kα)/cm^{-1}	34.526	146.47
Diffractometer	Philips PW 1100	Enraf Nonius CAD4
T/°C	22	22
Unique total data	11568	13265
Unique observed data [$I > 2\sigma(I)$]	6957 (R_{int} = 0.022)	6450 (R_{int} = 0.031)
R, *R*1	*R* = 0.0354	*R*1 = 0.0824 (0.1665, all data)
R′, *wR*2	*R*′ = 0.0447	*wR*2 = 0.2343 (0.3416, all data)

Table 2 Selected bond distances (Å) and angles (°) for compound **2**·MeOH

Ru(1)–Ru(2)	2.793(1)	Ru(2)–C(4)	1.888(6)
Ru(1)–Ru(4)	2.852(1)	Ru(3)–Ru(4)	2.772(1)
Ru(1)–Se(1)	2.544(1)	Ru(3)–Se(1)	2.582(1)
Ru(1)–Se(2)	2.604(1)	Ru(3)–Se(2)	2.608(1)
Ru(1)–P(1)	2.304(1)	Ru(3)–C(7)	2.051(6)
Ru(1)–C(2)	1.877(5)	Ru(4)–Se(1)	2.626(1)
Ru(2)–Ru(3)	2.855(1)	Ru(4)–Se(2)	2.586(1)
Ru(2)–Se(1)	2.580(1)	Ru(4)–C(7)	2.042(5)
Ru(2)–Se(2)	2.561(1)	P(1)–C(10)	1.836(5)
Ru(2)–P(2)	2.341(1)	P(2)–C(10)	1.841(5)
Se(1)–Ru(1)–P(1)	155.5(1)	Ru(1)–Ru(4)–C(7)	137.5(2)
Se(1)–Ru(1)–Se(2)	79.6(1)	Se(1)–Ru(4)–Se(2)	78.5(1)
Ru(4)–Ru(1)–P(1)	132.5(1)	Ru(2)–Se(1)–Ru(4)	100.1(1)
Ru(2)–Ru(1)–C(2)	162.8(2)	Ru(1)–Se(1)–Ru(3)	101.9(1)
Ru(2)–Ru(1)–Ru(4)	89.9(1)	Ru(2)–Se(2)–Ru(4)	101.7(1)
Ru(1)–Ru(2)–Ru(3)	89.6(1)	Ru(1)–Se(2)–Ru(3)	99.6(1)
Se(1)–Ru(2)–P(2)	144.5(1)	Ru(1)–P(1)–C(10)	109.3(2)
Se(1)–Ru(2)–Se(2)	79.8(1)	Ru(2)–P(2)–C(10)	113.5(2)
Ru(1)–Ru(2)–C(4)	155.8(2)	Ru(4)–C(7)–O(7)	138.6(5)
Ru(3)–Ru(2)–P(2)	141.0(1)	Ru(3)–C(7)–O(7)	136.1(4)
Ru(2)–Ru(3)–C(7)	137.5(2)	Ru(3)–C(7)–Ru(4)	85.3(2)
Ru(2)–Ru(3)–Ru(4)	90.3(1)	P(1)–C(10)–P(2)	115.2(2)
Se(1)–Ru(3)–Se(2)	78.9(1)	Ru(1)–C(2)–O(2)	172.9(4)
Ru(1)–Ru(4)–Ru(3)	90.1(1)	Ru(2)–C(4)–O(4)	170.3(5)

Table 3 Selected bond distances (Å) and angles (°) for compound **4**·CH_2Cl_2

Ru(1)–Ru(2)	3.023(3)	Ru(4)–Se(3)	2.501(3)
Ru(1)–Ru(5)	3.002(2)	Ru(4)–Se(4)	2.525(3)
Ru(1)–Se(1)	2.506(3)	Ru(4)–P(3)	2.319(5)
Ru(1)–Se(2)	2.522(2)	Ru(5)–Ru(6)	2.826(2)
Ru(1)–P(1)	2.321(6)	Ru(5)–Se(3)	2.456(3)
Ru(2)–Ru(3)	2.812(2)	Ru(5)–Se(4)	2.512(3)
Ru(2)–Ru(4)	2.983(2)	Ru(6)–Se(3)	2.488(3)
Ru(2)–Ru(5)	2.857(2)	Ru(6)–Se(4)	2.509(2)
Ru(2)–Se(1)	2.457(3)	Ru(6)–P(4)	2.307(5)
Ru(2)–Se(2)	2.529(3)	C(13)–P(1)	1.84(2)
Ru(3)–Se(1)	2.493(3)	C(13)–P(2)	1.88(2)
Ru(3)–Se(2)	2.508(3)	C(14)–P(3)	1.83(2)
Ru(3)–P(2)	2.311(6)	C(14)–P(4)	1.80(2)
Ru(4)–Ru(5)	3.014(2)		
Se(1)–Ru(1)–Se(2)	81.7(1)	Ru(1)–Ru(5)–Ru(4)	111.9(1)
Ru(5)–Ru(1)–P(1)	170.4(1)	Ru(1)–Ru(5)–Ru(2)	62.0(1)
Ru(2)–Ru(1)–P(1)	129.5(2)	Ru(4)–Ru(5)–Ru(6)	78.6(1)
Ru(2)–Ru(1)–Ru(5)	56.6(1)	Ru(2)–Ru(5)–Ru(6)	138.7(1)
Ru(1)–Ru(2)–Ru(5)	61.3(1)	Ru(1)–Ru(5)–Ru(6)	135.3(1)
Ru(1)–Ru(2)–Ru(4)	112.3(1)	Se(3)–Ru(5)–Se(4)	82.7(1)
Ru(1)–Ru(2)–Ru(3)	78.8(1)	Ru(5)–Ru(6)–P(4)	138.8(1)
Se(1)–Ru(2)–Se(2)	82.5(1)	Se(3)–Ru(6)–Se(4)	82.2(1)
Ru(4)–Ru(2)–Ru(5)	62.1(1)	Ru(1)–Se(1)–Ru(3)	95.8(1)
Ru(3)–Ru(2)–Ru(5)	138.7(1)	Ru(1)–Se(2)–Ru(3)	95.0(1)
Ru(3)–Ru(2)–Ru(4)	132.7(1)	Ru(4)–Se(3)–Ru(6)	95.8(1)
Ru(2)–Ru(3)–P(2)	138.7(2)	Ru(4)–Se(4)–Ru(6)	94.7(1)
Se(1)–Ru(3)–Se(2)	82.2(1)	P(1)–C(13)–P(2)	118(1)
Ru(2)–Ru(4)–P(3)	169.5(1)	P(3)–C(14)–P(4)	123(1)
Ru(2)–Ru(4)–Ru(5)	56.9(1)	Ru(1)–P(1)–C(13)	115.6(6)
Se(3)–Ru(4)–Se(4)	81.6(1)	Ru(3)–P(2)–C(13)	111.4(7)
Ru(5)–Ru(4)–P(3)	129.6(2)	Ru(4)–P(3)–C(14)	115.7(6)
Ru(2)–Ru(5)–Ru(4)	61.0(1)	Ru(6)–P(4)–C(14)	113.4(7)

the strongest ones being C(13)···O(6) 3.26(1) Å, C(13)–H(13)···O(6) 123.3(5)° and C(30)–O(5) 3.36(1) Å, C(37)–H(30)···O(5) 125.4(5)° involving aromatic CH groups and carbonyl oxygens, and C(10)···O(10) 3.41(1) Å, C(10)–H(10)···O(10) 144.6(5)° involving the dppm methylene bridge and the methanol oxygen.

The pyrolysis of compound **1** in toluene solution, in the presence of Me_3NO, affords the new hexanuclear cluster [$Ru_6(\mu_3$-$Se)_4(CO)_{12}(\mu$-dppm$)_2$] **4**. The structure of its dichloromethane solvate has been fully elucidated by X-ray diffraction. A view of the structure of **4** is shown in Fig. 3 together with the atomic numbering scheme. Selected bond distances and angles are given in Table 3. Cluster **4** may be thought of as derived by the condensation of two [$Ru_3(\mu_3$-$Se)_2(CO)_6$(dppm)] units formed by the loss of a CO ligand from the apical metal atom of **1**. Three new metal–metal bonds join the two triruthenium diselenido fragments.

Compound **4** has the same cluster geometry as that of [$Os_6(\mu_3$-$S)_4(CO)_{16}$], obtained from [$Os_3(\mu_3$-$S)_2(CO)_9$] by photolysis.[14] It consists of a central butterfly Ru_4 core surrounded by two 6-electron L_3RuSe_2 moieties. The presence of ten 2-electron ligands (L) fixes the electron count for this Ru_4 core at 64e, *i.e.* two electrons in excess of the predicted count according to the EAN rule expectation for a butterfly geometry. This cluster core is therefore a member of the growing class of electron rich M_4 systems which possess interesting structural features and chemical reactivity.[15] Moreover, this Ru_6 cluster with 96 cluster valence electrons should possess only 6 Ru–Ru bonds. Therefore with 7 Ru–Ru interactions the cluster as a whole is electron rich. This "richness" is principally associated with electron density in MOs antibonding with respect to the central Ru_4 core, as proposed by Adams and Horwáth[14] for the hexaosmium derivative. This could account for the lengthening of the four perimetrical Ru–Ru bond distances of the butterfly core ranging from 2.983(2) to 3.023(3) Å, whereas the hinge and the two peripheral Ru–Ru bonds range from 2.811(2) to 2.858(2)Å.

The dihedral butterfly angle between the averaged planes Ru(1), Ru(2), Ru(5) and Ru(2), Ru(4), Ru(5) is 141.1(1)°, in such a way that the Se(2) atom approaches Se(4) to 3.517(3) Å. The short bite of the dppm ligands [averaged P · · · P distance 3.19(1) Å; P–C–P angle 121(1)°] causes the approach of the co-ordinated ruthenium atoms [Ru(1) · · · Ru(3) 3.709(2) Å, Ru(4) · · · Ru(6) 3.702(2) Å] considering that the corresponding distance in $[Ru_3(\mu_3\text{-}Se)_2(CO)_7(PPh_3)_2]$[1e] is 3.844(2) Å. In parallel, the Se · · · Se distances rise from 3.208(2) Å in $[Ru_3(\mu_3\text{-}Se)_2(CO)_7(PPh_3)_2]$ to 3.288(3) and 3.284(3) Å in **4**.

The methylene carbons of the dppm ligands C(13) and C(14) approach Se(1) and Se(2) respectively to 3.34(2) and 3.41(2) Å. Correspondingly the two hydrogen atoms from the CH_2 groups experience two different environments giving two NMR doublets of triplets, well distinguishable even at room temperature. Also in this case a lot of C–H · · · O interactions involving aromatic C–H groups and carbonyl oxygens of adjacent molecules [C · · · O distances ranging from 3.20(3) to 3.60(3) Å] appear to contribute to the packing.

Acknowledgements

Financial support from Ministero dell'Università e della Ricerca Scientific & Tecnologica (Rome) is gratefully acknowledged.

References

1 (*a*) G. Hogarth, N. J. Taylor, A. J. Carty and A. Meyer, *J. Chem. Soc., Chem. Commun.*, 1988, 834; (*b*) F. Van Gastel, L. Agocs, A. A. Cherkas, J. F. Corrigan, S. Doherty, R. Ramachandran, N. J. Taylor and A. J. Carty, *J. Cluster Sci.*, 1991, **2**, 131; (*c*) S. M. Stuczynski, Y.-U. Kwon and M. L. Steigerwald, *J. Organomet. Chem.*, 1993, **449**, 167; (*d*) W. Imhof and G. Huttner, *J. Organomet. Chem.*, 1993, **448**, 247; (*e*) P. Baistrocchi, D. Cauzzi, M. Lanfranchi, G. Predieri, A. Tiripicchio and M. Tiripicchio Camellini, *Inorg. Chim. Acta*, 1995, **235**, 173.

2 M. L. Steigerwald, T. Siegrist, E. M. Gyorgy, B. Hessen, Y.-U. Kwon and S. M. Tanzler, *Inorg. Chem.*, 1994, **33**, 3389.

3 (*a*) B. F. G. Johnson, T. M. Layer, J. Lewis, A. Martin and P. R. Raithby, *J. Organomet. Chem.*, 1992, **429**, C41; (*b*) T. M. Layer, J. Lewis, A. Martin, P. R. Raithby and W.-T. Wong, *J. Chem. Soc., Dalton Trans.*, 1992, 3411; (*c*) P. Mathur, Md. M. Hossain and R. S. Rashid, *J. Organomet. Chem.*, 1993, **460**, 83; (*d*) P. Mathur, B. H. S. Thimmappa and A. L. Rheingold, *Inorg. Chem.*, 1990, **29**, 4658; (*e*) P. Mathur, Md. M. Hossain and R. S. Rashid, *J. Organomet. Chem.*, 1993, **448**, 211.

4 D. Cauzzi, C. Graiff, M. Lanfranchi, G. Predieri and A. Tiripicchio, *J. Organomet. Chem.*, 1997, **536–537**, 497.

5 D. Cauzzi, C. Graiff, M. Lanfranchi, G. Predieri and A. Tiripicchio, *J. Chem. Soc., Dalton Trans.*, 1995, 2321.

6 A. M. Z. Slawin, M. B. Smith and J. D. Woollins, *J. Chem. Soc., Dalton Trans.*, 1997, 1877.

7 A. M. Bond, R. Colton and P. Panagioridou, *Organometallics*, 1988, **7**, 1767.

8 N. Walker and D. Stuart, *Acta Crystallogr., Sect. A*, 1983, **39**, 158; F. Ugozzoli, *Comput. Chem.*, 1987, **11**, 109.

9 G. M. Sheldrick, SHELXS 86, Program for the Solution of Crystal Structures, Universität Göttingen, 1986.

10 G. M. Sheldrick, SHELX 76, Program for Crystal Structure Determination, University of Cambridge, 1976.

11 G. M. Sheldrick, SHELXL 93, program for the refinement of crystal structures, University of Göttingen, 1993.

12 E. J. Houser, A. Venturelli, T. B. Rauchfuss and S. R. Wilson, *Inorg. Chem.*, 1995, **34**, 6402.

13 P. Baistrocchi, M. Careri, D. Cauzzi, C. Graiff, M. Lanfranchi, P. Manini, G. Predieri and A. Tiripicchio, *Inorg. Chim. Acta*, 1996, **252**, 367.

14 R. D. Adams and I. T. Horwáth, *J. Am. Chem. Soc.*, 1984, **106**, 1869.

15 J. F. Corrigan, Y. Sun and A. J. Carty, *New J. Chem.*, 1994, **18**, 77.

Paper 8/06940I